Physical Properties of *Escherichia coli* P Pili Measured by Optical Tweezers

Jana Jass,* Staffan Schedin,† Erik Fällman,‡ Jörgen Ohlsson,§ Ulf J. Nilsson,§ Bernt Eric Uhlin,¶ and Ove Axner‡

*Department of Microbiology and Immunology, The Lawson Health Research Institute, University of Western Ontario, London, Ontario, N6A 4V2, Canada; †Department of Applied Physics and Electronics, and ‡Department of Physics, Umeå University, SE-901 87 Umeå, Sweden; §Organic and Bioorganic Chemistry, Lund University, SE-221 00 Lund, Sweden; and ¶Department of Molecular Biology, Umeå University, SE-901 87 Umeå, Sweden

ABSTRACT The mechanical behavior of individual P pili of uropathogenic *Escherichia coli* has been investigated using optical tweezers. P pili, whose main part constitutes the PapA rod, composed of $\sim 10^3$ PapA subunits in a helical arrangement, are distributed over the bacterial surface and mediate adhesion to host cells. They are particularly important in the pathogenesis of *E. coli* colonizing the upper urinary tract and kidneys. A biological model system has been established for in situ measurements of the forces that occur during mechanical stretching of pili. A mathematical model of the force-versus-elongation behavior of an individual pilus has been developed. Three elongation regions of pili were identified. In region I, P pili stretch elastically, up to a relative elongation of 16 ± 3%. The product of elasticity modulus and area of a P pilus, *EA*, was assessed to 154 ± 20 pN ($n = 6$). In region II, the quaternary structure of the PapA rod unfolds under a constant force of 27 ± 2 pN ($n \approx 100$) by a sequential breaking of the interactions between adjacent layers of PapA subunits. This unfolding can elongate the pilus up to 7 ± 2 times. In region III, pili elongate in a nonlinear manner as a result of stretching until the bond ruptures.

INTRODUCTION

Adhesion of bacteria to host tissue is an essential step in the progression of an infection. Bacterial pili are responsible for mediating adhesion and maintaining bacteria-host contact during the initial stages of an infection by many Gram-negative bacteria. Uropathogenic *Escherichia coli*, which are implicated in 75–80% of uncomplicated urinary tract infections and in severe pyelonephritis, express a variety of different fimbrial adhesins of which P pili predominantly are expressed by isolates from the upper urinary tract (Johnson and Russo, 2002; Russo and Johnson, 2003). Thus P pili, expressed by ~90% of the *E. coli* strains that cause pyelonephritis (upper urinary tract and kidney infections), constitute an important virulence factor (Källenius et al., 1981).

E. coli colonizing the urinary tract are exposed to mechanical host defenses, including urine flow, that create shear forces. These shear forces cause the bacterium-host distance to be dissimilar at different parts of the binding area, resembling the ''unzipping'' of Velcro (Liang et al., 2000). Presumably to withstand such forces, P pili have evolved into a three-dimensional helix-like structure that can be successively unfolded when exposed to increasing urine flow (Bullitt and Makowski, 1998, 1995; Gong and Makowski, 1992, 1990; Gong et al., 1992). This unfolding mechanism allows a single pilus to support tension over a broad range of lengths, which in turn makes it possible for a large number of pili to support tension simultaneously (Bullitt and Makowski 1998, 1995). The flexible structure of the P pili thus makes *E. coli* capable of withstanding considerable shear forces so as to stay attached to the host tissue under a variety of conditions.

Individual P pili have previously been characterized with respect to their protein composition and static structure (sizes and three-dimensional shape). As depicted in Fig. 1, P pili constitute a long helical rod of ~6.8 nm in diameter, with a short (15 nm), thin (2–3 nm) flexible fibrillum tip (Bullitt and Makowski, 1998). The major subunit, PapA, held together by hydrophobic interactions of a single β-strand in a motif that is reinforced by a coiled configuration, makes up the pilus rod (Bullitt et al., 1996). The pilus is anchored to the membrane by PapH (Båga et al., 1987) and connected to the fibrillum by the adaptor, PapK (Lindberg et al., 1986). The fibrillum, in turn, is a thin flexible structure composed of noncovalently linked minor subunits, PapE (Lindberg et al., 1986), PapF (Lindberg et al., 1986), and the adhesin PapG (Jacob-Dubuisson et al., 1993; Kuehn et al., 1992; Lindberg et al., 1987). Inasmuch as the major subunit of the P pilus is PapA, most of the mechanical (physical) properties of the pilus should then be governed by the properties of the PapA rod.

The mechanical properties of P pili have not been assessed in detail previously. This is primarily due to the requirement of sophisticated techniques that can simultaneously measure the weak forces in the low piconewton range and minute elongation distances in the nanometer range that are involved in the stretching of pili. Such technology has only recently become available. Among the various new techniques that have been developed for measuring minute forces and

Submitted April 23, 2004, and accepted for publication September 14, 2004.

Address reprint requests to Ove Axner, E-mail: ove.axner@physics.umu.se.

0006-3495/04/12/4271/13 $2.00

doi: 10.1529/biophysj.104.044867

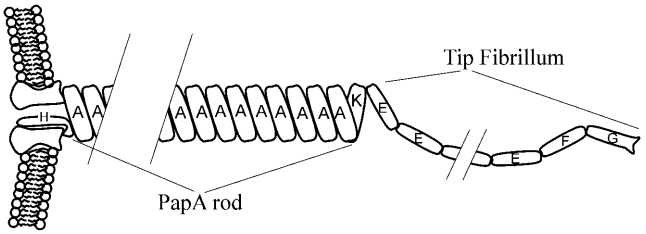

FIGURE 1 Schematic illustration of a P pilus (adapted from Bullitt et al., 1996). The major component is composed of ~1000 PapA subunits that form a thin (6.8 nm in diameter) ~1-μm-long right-handed helical rod (the PapA rod) with 3.28 subunits per turn. The PapA rod is anchored to a bacterial membrane by PapH and connected to a fibrillum by a PapK adaptor. The fibrillum tip (15-nm long and 2–3 nm in diameter) is a flexible structure composed of PapE, PapF, and the PapG adhesin.

distances, atomic force microscopy (AFM) (Cappella and Dietler, 1999; Chen and Moy, 2002; Giocondi et al., 2003; Hansma and Pietrasanta, 1998; Ikai and Afrin, 2003; Kumar and Hoh, 2001; Stolz et al., 2000; Tromas and Garcia, 2002; Willemsen et al., 2000; Zlatanova et al., 2000) and optical tweezers (OT) (Gallet, 2004; Kuo, 2001; Kuyper and Chiu, 2002; Rice et al., 2003; Svoboda and Block, 1994) are the most suitable for biological applications (Leckband, 2000; Leckband and Israelachvili, 2001; Merkel, 2001). Although both techniques have been used for investigating receptor-ligand interactions, OT have the advantage of higher resolution in the low piconewton range. OT have therefore been used for experiments such as characterization of physical properties of DNA (Bustamante et al., 2003).

The OT technique also allows interactions to be measured in situ, consequently the measurements can be performed on living bacteria or cells. The technique has therefore been used for studies of mechanical properties of bacterial fiber structures. For example, Liang et al. (2000) investigated the binding of *E. coli* type 1 pili to specific mannose moieties incorporated into self-assembled monolayers at various concentrations. Merz et al. (2000) and Maier et al. (2002) investigated the retraction of type IV pili of *Neisseria gonorrhea* involved in surface motility. OT have also been used to study the flagella rotary motor of *E. coli* (Berry and Berg, 1997; Chen and Berg, 2000). In this article, we extend the applications of OT to investigate the mechanical properties of pili using the P pili as a model system.

We have examined the mechanical elongation properties of P pili using OT; specifically, the elastic elongation and the unfolding process of the three-dimensional structure of the PapA rod that takes place under exposure to external forces. Furthermore, various inherent material entities that these pili possess have been determined, including the stiffness and elasticity modulus for the elastic elongation of P pili and the force required for unfolding of the helix-like PapA rod. By applying a meticulous calibration procedure, emphasis has been given to provide absolute values to the measured entities.

To avoid possible interference of other similar (i.e., fimbrial) surface structures, the P pili were expressed in the otherwise afimbriated *E. coli* strain HB101 from the plasmid pPAP5. To validate that the measurements were indeed of P pili, control experiments were performed both on P pili expressed from HB101/pPAN5, whose pili length is considerably shorter than those of HB101/pPAP5, and on free pili. Furthermore, the measurements have been performed both under low and high loading rates (from a few piconewtons per second to several hundreds of piconewtons per second) to investigate any possible influence of the loading rate. The measurements provided a general characterization of the mechanical properties of an individual P pilus, primarily the contributions from the PapA rod, as well as the force-versus-elongation characteristics of binding mediated by several P pili simultaneously.

MATERIALS AND METHODS

Bacteria and culture conditions

Two recombinant derivatives of *E. coli* HB101 were used to express the P pili. The HB101/pPAP5 carries the entire *pap* gene cluster on the vector pBR322 and expresses normal P pili (Lindberg et al., 1984), whereas HB101/pPAN5 carries a mutant *pap* gene cluster that expresses fewer PapA subunits and shorter P pili due to a deletion in the region important for posttranscriptional mRNA processing and differential gene expression in the operon (Nilsson et al., 1996). The bacteria were cultured on trypticase soy agar (TSA, Difco, Sparks, MD), supplemented with 50 μg/ml carbenicillin (Sigma, St. Louis, MO) at 37°C overnight and resuspended in phosphate buffered saline, pH 7.4 (PBS) just before use.

Hemagglutination was used to confirm the expression of pili in the cultures before the force measurements. Heparinized rabbit blood was washed in PBS and diluted to 8% red blood cells. Overnight bacterial cultures were resuspended in 10 μl PBS on a glass plate, 10 μl of red blood cells were added, and the suspension was gently mixed while maintained on ice.

Isolation of Pili

P pili were purified according to a modified procedure of Gong and Makowski (Gong et al., 1992). Briefly, *E. coli* HB101/pPAP5, grown overnight on TSA at 37°C, were harvested and resuspended in 20 ml cold 5 mM Tris-HCl solution (pH 8.0). The pili were sheared with a homogenizer, and cells and debris were centrifuged. The pili were precipitated overnight with ammonium sulfate (55%) and collected by centrifugation. The pili were washed three times with 0.5 mM Tris-HCl (pH 7.5), resuspended in the same buffer, and dialyzed overnight. The pili were centrifuged again and filtered through a 0.2-μm low-protein binding filter (MILLEX-GV).

Optical tweezers

The optical tweezers system was constructed around an inverted microscope (Olympus IX70, Olympus, Melville, NY) with a high numerical aperture oil-immersion objective. The trapping laser was an argon ion laser-pumped continuous-wave titanium-sapphire laser, operated at 810 nm. A complete description of the optical arrangement has previously been given (Fällman and Axner, 1997).

The basic principle for force measurements by the optical tweezers technique can be summarized as follows. The restoring force on a bead in

a trap created by optical tweezers is, for a small spherical bead and for displacements less than half the radius of the bead, linearly proportional to the position of the bead in the trap (Ashkin, 1992). A small particle held by the optical tweezers will therefore shift its position in the trap an amount that is proportional to any external force to which it is exposed. The force exerted onto a trapped bead at any moment in time can thereby be determined by monitoring the displacement of the bead in the trap.

The trapping force in OT is typically in the lower piconewton range (from a single piconewton to hundreds of piconewtons), depending on the intensity and shape of the laser beam, the numerical aperture of the objective, the amount of aberrations in the optical system, and the size, shape, and refraction index of the trapped particle. The use of a spherical, nondeformable object as the ''handle'' in the trap, such as a bead, is a prerequisite for a linear force-versus-displacement relation in the trap.

The position of a transparent spherical object in the trap can conveniently be monitored by the use of a probe laser, which in our system was a stabilized HeNe laser with an intensity set to a fraction of the trapping beam to prevent interference with the balance of forces in the system. The probe beam is focused a short distance below the trapped bead in such a way that the bead focuses the light to a distinct spot in the far field where a position sensitive detector is placed to monitor the position of the probe beam spot. The signals from the detector are amplified via a preamplifier, followed by digitalization and sampling by a data acquisition card. A detailed description of the arrangement for conveying the probe laser beam into the microscope is given in Fällman et al. (2004).

Before each measurement, the stiffness of the optical trap (defined as the derivative of the force with respect to distance for a small particle in the trap) was assessed using a calibration technique based upon the power spectrum of the Brownian motion of the trapped particle (Berg-Sorensen and Flyvbjerg, 2004; Svoboda and Block, 1994). The main advantage of this technique is that it can be performed rapidly in situ; a typical calibration procedure takes only a few seconds. A calibration can therefore be done before each measurement. To validate the Brownian motion calibration technique, separate calibrations were performed based upon the Stoke drag force (Svoboda and Block, 1994). The two calibration techniques were found to concur to within a few percent.

Typical stiffness values of the optical trap were in the 0.03–0.3 pN/nm range, which corresponded to a laser power of from 150 mW to 1.5 W measured directly after the laser. The separation velocity for the measurements reported here was 0.5 μm/s. This implies that the loading rates were in the range between 15 and 150 pN/s. Separate measurements with significantly lower loading rates (in the order of 1 pN/s) were also performed but did not yield any significantly different data.

Measurement principle

The measurements were performed through an ordered sequence of actions. Using the OT, a suspended bacterium was mounted onto a large bead that was secured to the coverslip via a hydrophobic interaction. A smaller bead was captured by the OT and brought into contact with the bacterial pili. The smaller bead served two simultaneous purposes; it provided a surface to which the pili could bind and it constituted the handle for the force measurements. The large bead was then moved from the trap while the forces mediated by the pili, acting onto the small bead, were measured by monitoring the displacement of the smaller bead in the trap (Fällman et al., 2004).

Preparation of coverslips and beads

Glass coverslips were washed thoroughly, cleaned, and silanized with 10% dimethyldichlorosilane (Sigma) in trichloroethylene according to the procedure of Otto et al. (1999) to make them hydrophobic. The silanized coverslips were washed vigorously in ethanol and stored in ethanol. Just before use, the coverslips were dried and placed into a holder.

The large beads onto which the bacteria were mounted were 9.6 μm carboxyl latex beads (Interfacial Dynamics, Portland, OR). The bacterium and the purified pili were coupled to the carboxylic acid groups on the bead using 1-ethyl-3-(3-dimethylaminopropyl) carbodiimide hydrochloride (EDAC) and *N*-hydroxysuccinimide (NHS) to produce unstable NHS esters that subsequently react with the primary amino groups on bacterial surface proteins (Staros et al., 1986). Briefly, the beads were washed in 0.025 M MES buffer, pH6.0 (Sigma), and resuspended to 20 mg/ml solids. To activate the beads, 25 μl of washed beads were resuspended in 1.0 ml of activation buffer (0.1 M MES, 0.5M NaCl, pH 5.0). EDAC (0.4 mg) and NHS (0.6 mg) were added to the suspension and incubated at room temperature for 20–30 min. Beads were washed, resuspended in 50 μl activation buffer, and stored at 4°C to be used within 1 day of preparation. Bacteria and purified pili were covalently bound to the beads when the pH increased from 5 to 7.4, destabilizing the reactive amine intermediate.

The small beads onto which the pili bound, and that also served the purpose of a handle for the OT, were 3 μm in diameter and consisted of hydrophobic latex (Interfacial Dynamics). The beads were functionalized with α-D-galactopyranosyl-(1$\rightarrow$4)-β-D-galactopyranoside for a separate study of the receptor-mediated adhesion properties of P pili. However, in this study the beads functioned as a surface onto which pili could bind unspecifically through the inherent hydrophobicity of the bead. This functionalization, which is described elsewhere (E. Fällman, M. Andersson, J. Jass, S. Schedin, J. Ohlsson, U. J. Nilsson, B. E. Uhlin, and O. Axner, unpublished data), is therefore believed not to have any influence on the study of the mechanical properties of P pili presented in this work.

Sample preparation and detailed measurement procedure

Samples were prepared directly on the silanized coverslip by sequentially adding 25 μl freshly resuspended *E. coli* in PBS, 5 μl activated 9.6-μm beads, and 5 μl small beads in PBS. Another coverslip was placed on top separated by a spacer and placed onto the microscope.

The activated 9.6-μm beads migrated and bound to the coverslip within a few minutes. A bacterium was captured by the OT at low power and mounted onto the large bead as is schematically illustrated in Fig. 2 *A*. The bacterium was held at this position until the reaction was considered complete (up to a few seconds). To ensure that the bacterium was strongly linked to the large bead, attempts were made to move it using the OT, and only those bacteria that remained fully immobilized were used for the force measurements.

Next, a suspended small bead was trapped by the optical tweezers. The trap was then calibrated before the bead was brought into contact with the bacterium (Fig. 2 *B*). A strong bond was formed, primarily originating from nonspecific hydrophobic forces present between the pili and the bead.

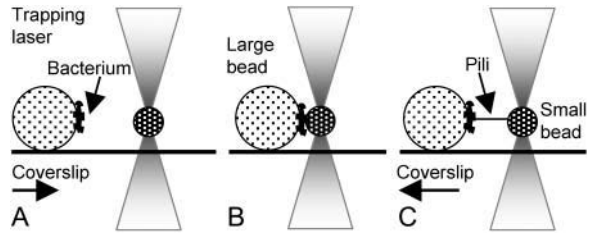

FIGURE 2 Measurement procedure. (*A*) A bacterium is mounted onto the 9.6-μm activated bead attached to the coverslip. The trapped bead serves both as a surface onto which the bacterial pili bind and as a force indicator in the optical tweezers system. (*B*) The trapped bead is moved close to the bacterium forming a strong bond between the bacterial pili and the bead. (*C*) A force is exerted on the pili by moving the coverslip with the large bead. The displacement of the trapped bead is thereby a measure of the exerted force.

As illustrated in Fig. 2 *C*, a force can be exerted on the pilus/pili bound to the small bead by moving the coverslip, and thereby the large bead together with the bacterium, away from the trapped bead. As the force was increased, the position of the small bead became displaced a small distance relative to the center of the trap. Inasmuch as the force in an OT is (for small displacements) proportional to the distance from the center of the trap, the displacement of the small bead constituted a measure of the force exerted on the small bead by the bacterium, mediated by the pili. The position of the small bead was therefore continuously monitored until the binding ruptured, providing continuous information of the force variation as a function of position of the large bead, which in turn could be related to the length of the pilus.

Atomic force microscopy

Bacteria and purified pili were examined using AFM. Bacteria were resuspended in sterile water (MilliQ) and 5 μl were placed on a freshly cleaved mica surface. After 5-min incubation at room temperature, the bacteria were rinsed once with 10 μl of the sterile water, blotted dry, and placed into a desiccator for 1 h. The samples were imaged with a MultiMode Nanoscope IIIa in TappingMode (Digital Instruments, Santa Barbara, CA) using standard silicon cantilevers at resonant frequency of 270–310 kHz. Images were collected at a scan rate of 0.5–1.2 Hz at 512-sample resolution. The final images were presented in either height mode or amplitude mode (error mode) after flattening and/or plane fitting using Digital Instruments software. Measurements of structures in the *z*-direction were done using the height mode.

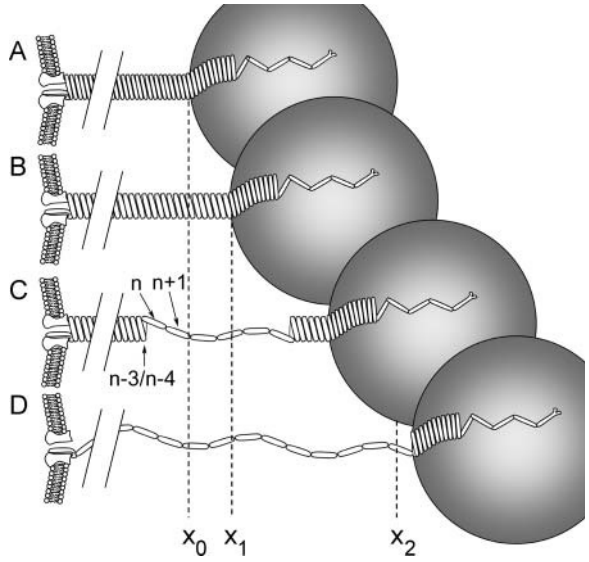

FIGURE 3 Schematic illustration of the three elongation regions of a P pilus. (*A*) A P pilus in its unstretched mode attached to a bead. (*B*) A P pilus fully stretched in region I. (*C*) A P pilus in its elongation region II. (*D*) A P pilus elongated in region III. x_0, x_1, and x_2 represent the length of an unstretched P pilus that mediates the binding, the length at which the pilus passes from region I to region II, and the length at which the pilus passes from region II to region III, respectively. Panel *C* displays the unfolding process in which the binding between the nth and the $(n-3)$th and/or $(n-4)$th PapA subunits in the adjacent layer has been broken.

THEORY

Modeling the physical properties of a pilus

It is possible to construct a simple model of the physical properties of a pilus based upon the most distinguishing features of the experimental findings. In short, as is shown below, the first effect of pilus extension is elastic stretching, possibly originating from an elongation of the interactions between adjacent turns of the helix or an elongation or reorientation of the subunits themselves. The region in which this elastic elongation occurs is referred to as region I. As the extension distance is increased, the interactions between adjacent turns of the helix of the PapA subunits start to break in a serial manner, resulting in an unfolding of the quaternary, helix-like structure. This elongation region is denoted region II. When the entire PapA rod has been unfolded, finally, the pilus enters a third region of elongation, in which either the head-to-tail interaction angle between subsequent PapA subunits is increased or the PapA subunits themselves are being elongated (or a combination of the two). This region of elongation is referred to as region III. The three elongation regions are schematically depicted in Fig. 3.

A simple mathematical model for the force-versus-elongation (or length) response of a single pilus, $F_p(x)$, can be created from a few simple assumptions. The first assumption is that the initial elastic elongation of the pilus can be described as the elongation of a linear spring. This implies that the force response in region I, $F_I(x)$, can be written in terms of a product of a stiffness, k_p, and the elongation of the pilus, $x - x_0$, where x and x_0 are the length of the pilus that mediates the binding in the presence and absence of any forces, respectively. The second assumption is that there is a successive breaking of the interactions between adjacent layers of subunits in the PapA rod in region II. As has been discussed by Bullit et al. (1996), the rod has 3.28 PapA subunits per turn. Disruption of the interactions between adjacent layers implies a serial breaking of the nth and the $(n-3)$th and/or $(n-4)$th subunits in the PapA rod (where nth represents the outermost PapA subunit in the last turn of the folded part of the helix and the $(n-3)$th and $(n-4)$th subunits belong to the second last turn of the folded part of the helix), as is illustrated in Fig. 3 *C*. This leads to the conclusion that the unfolding should occur under a constant force. The force response in region II, F_{II}, will therefore simply be denoted by F_{uf}. As observed in the experiments, the force-versus-elongation relationship for the third region has a more complex form. It suffices in this model to simply refer to it as $F_{III}(x)$. In conclusion, this implies that a simple mathematical model of the total force-versus-elongation response for a single pilus, $F_p(x)$, can be expressed as:

$$F_p(x) = \begin{cases} 0 & x \le x_0 \quad \textit{Before stretching} \\ F_I(x) = k_p(x - x_0) & x_0 \le x \le x_1 \quad \textit{Region I} \\ F_{II} = F_{uf} & x_1 \le x \le x_2 \quad \textit{Region II} \\ F_{III}(x) & x_2 \le x \quad \textit{Region III} \end{cases}, \tag{1}$$

where, thus, x represents the distance between the bacterium and the surface to which the pilus bound (the small bead) and x_0 the unstretched length of the part of the pilus that mediates the binding (equal to the distance between the bacterium and the trapped bead when the binding starts to take up force) (see Fig. 3). x_1 and x_2 are the bacterium-bead distances at which the pilus passes from region I to region II, and from region II to region III, respectively. A typical form of the force response of a single pilus, according to the model given above, is schematically depicted in Fig. 4. We have here, for schematic purposes, given the force response in region III the form of an ''s'', inasmuch as this is in qualitative agreement with the experimental findings.

Although convenient from a phenomenological point of view (the stiffness equals the slope of a force-versus-elongation curve), the concept of stiffness in region I is not as practical inasmuch as is shown below, its magnitude depends on the length of the part of the pilus mediating the binding (Fig. 3 *A*); a pilus binding with a longer length will have a smaller stiffness than one that binds with a shorter length. Inasmuch as pili have different natural lengths and non-specific binding can occur at various positions along the pilus, various pili will, therefore, in these types of measurements, show dissimilar stiffness and give rise to dissimilar slopes of their force-versus-elongation curves. For this reason, it has been found more appropriate to characterize a pilus in terms of an alternative length-independent ''material parameter''.

Borrowing concepts from the theory of elasticity, it can be concluded that it is possible to model a pilus in its linear elastic region as a rod-shaped entity with a given elasticity modulus (also referred to as the Young's modulus), E_p, (in units of N/m^2) and an ''area'' A_p (in units of m^2). The elasticity modulus for a one-dimensional material, E, is, in general, defined as the ratio of the tensile stress in a material, σ (in units of N/m^2), to its relative elongation, ε, i.e., as $\sigma = E\,\varepsilon$. Furthermore, the force in a rodlike material, F, (in units of N) is, in turn, related to the tensile stress through its area, A, as $F = \sigma A$. The force to which a pilus is exposed in region I, $F_I(x)$, can therefore be expressed as

$$F_I(x) = E_p A_p \varepsilon_p(x), \tag{2}$$

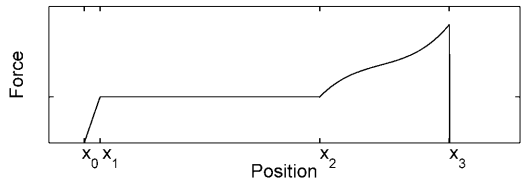

FIGURE 4 Predicted force-versus-position curve for a single pilus according to the model given in Eq. 1. x_0 is the length of the pilus in its unstretched mode, x_1 is the length at which it enters region II, x_2 is the length at which it enters region III, whereas x_3 represents the length at which the pilus detaches (or breaks).

where $\varepsilon_p(x)$ is the relative elongation of a pilus in region I.

However, inasmuch as a pilus does not have a (solid) rodlike structure, the modeling of a pilus as a rod provides a somewhat ambiguous measure of its area. The area A_p does not necessarily need to be seen as its ''true'' area, rather it should be seen as an ''associated'' area of the pili. The choice of area will affect the value of the elasticity modulus, E_p, however, only to such an extent that its product, E_pA_p, remains constant. It is, therefore, suitable to consider the product of E_p and A_p as a combined material entity, which for simplistic reasons will be written as $(EA)_p$ (expressed in units of N). This suggests that the force to which a pilus is exposed in region I, $F_I(x)$, can be expressed as

$$F_I(x) = (EA)_p \varepsilon_p(x) = (EA)_p (x - x_0)/x_0, \tag{3}$$

where we have used the fact $\varepsilon_p\,(x)$ can be expressed as $(x - x_0)/x_0$.

A comparison with the expression in Eq. 1 yields that the stiffness of a pilus, k_p, given by the slope of the force-versus-elongation curve from a single pilus, can be expressed in terms of a ratio of the product of the elasticity modulus and the ''area'', $(EA)_p$, and the length of a pilus mediating the binding, x_0, i.e., as

$$k_p = (EA)_p/x_0. \tag{4}$$

This also shows that the stiffness of a pilus in its linear elongation region, k_p, indeed depends on the length of the part of the pilus that mediates the binding, x_0, which, in turn, leads to the conclusion that the stiffness is not a suitable entity for characterization of the mechanical properties of P pili in region I. As will be discussed further below, this fact makes it difficult to determine the number of pili mediating the binding in region I solely from the slope of force-versus-elongation data.

Conversely, as is shown below, the unfolding force, F_{uf}, which appears as an elongation-independent force for a rather wide range of extensions (see below), can be directly and unambiguously determined from experimental data when the experimental system has been properly calibrated. Moreover, the unfolding force, F_{uf}, can be related to the product of the elasticity modulus and the ''area'' of a single pilus, $(EA)_p$, through the relative elongation of the pili in region I, $\varepsilon_p\,(x_1)$, which is defined as the relative elongation the pilus has undergone during its elastic stretching in region I, $(x_1 - x_0)/x_0$, according to

$$F_{uf} = \varepsilon_p(x_1)(EA)_p. \tag{5}$$

This comes from the fact that the transition from elastic elongation to unfolding for a single pilus shows up in a force-versus-elongation (or length) curve as a continuous transition from a straight line with a slope of k_p to the unfolding force

of a pilus in region II, F_{uf}, for a pilus length of x_1, which, according to Eq. 1, implies that $F_I(x_1) = F_{uf}$. Equation 5 then results as a consequence of Eq. 3.

Modeling the output of OT measurements

The output of the instrumentation (below referred to as raw data) provides, after appropriate calibration procedures, the total force in the bead-bacterium-bead system as a function of position of the large bead. The former is given by a measurement of the position of the small bead in the trap, whereas the latter is determined by the movement of the coverslip by a calibrated piezo stage. However, as the coverslip is being moved, and a force is being applied to the pili, the small bead (the handle) will shift its position in the trap. This implies that the elongation of the bond (or the part of the pili mediating the force) is not identical to the shift of the coverslip. To view the force data as a function of bond length and to assess some material properties of P pili, it is therefore necessary to consider the response of the entire bead-bacterium-bead model system.

The mechanical properties of our model system, with the small bead held by the optical tweezers and the large bead to which the bacterium was attached fastened on the coverslip, can be modeled by means of two symbolic springs as shown in Fig. 5. The spring attaching the small bead to the center of the trap (which is considered fixed) represents the stiffness of the trap, k_t, whereas the spring between the two beads, thus connecting the small bead to the bacterium, denoted by k_p, represents the stiffness of the bacterial binding. The displacement of the small bead from the center of the trap, which follows as a consequence of the force applied to the system, denoted by x_{SB}, has, in this figure, for reasons of clarity, been greatly exaggerated.

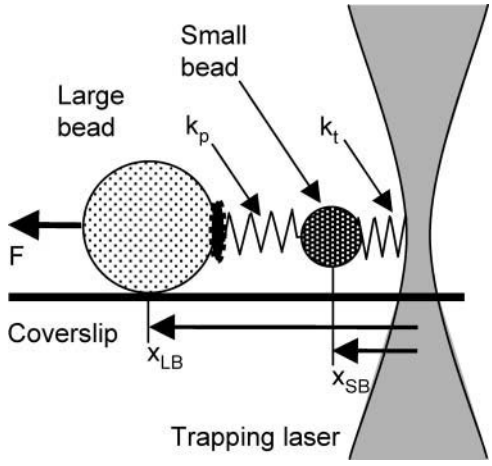

FIGURE 5 The model system idealized by two symbolic springs that represent the stiffness of the optical trap, k_t, and of the pili being stretched, k_p, respectively.

Inasmuch as the position of the small bead is not constant during a measurement, the output from the instrumentation, in the form of a force-versus-position curve, represents the force mediated by the two ''springs'' in response to the position of the large bead, x_{LB} (and not in response to the bacterium-to-small-bead-distance or the bond length). A force balance analysis of this system, modeling the stretching of one pilus within the linear elastic region (region I), provides a relation between the measured force in region I, F_I, the position of the large bead, x_{LB}, the position of the small bead in the trap, x_{SB}, (both measured with respect to the center of the trap), and the unstretched length of the free part of the pilus, x_0, according to

$$F_I(x_{LB}, x_{SB}, x_0) = k_p(x_{LB} - x_{SB} - x_0). \quad (6)$$

However, inasmuch as the position of the small bead in the trap, x_{SB}, depends on the force in the system (by the finite stiffness of the trap) according to

$$x_{SB} = F_I(x_{LB}, x_{SB}, x_0)/k_t, \quad (7)$$

the force balance expression above, Eq. 6, can be rewritten as a function solely depending on the position of the large bead according to

$$F_I(x_{LB}, x_0) = k_{eqv}(x_{LB} - x_0), \quad (8)$$

where we, for simplicity, have introduced an ''equivalent stiffness'', denoted by k_{eqv} and given by $k_{eqv} = (k_t^{-1} + k_p^{-1})^{-1}$. This equivalent stiffness, k_{eqv}, is, in fact, the stiffness for the system shown in Fig. 5 with the two symbolic springs coupled in series.

As was alluded to above, it is sometimes more convenient to display the measured force in terms of the actual length of the pilus, x, (rather than by the position of the large bead, x_{LB}); i.e., as

$$F_I(x) = k_p(x - x_0), \quad (9)$$

inasmuch as this has the advantage that the expression becomes independent of instrumental parameters (in this case the stiffness of the optical trap). The conversion of the raw data to a form that can provide the force as a function of pilus length, x, (equal to the actual bacterium-to-small-bead-distance, thus given by $x_{LB} - x_{SB}$) could be done by simply rescaling the x axis and plotting F_I versus the entity $x_{LB} - F_I/k_t$, inasmuch as the latter represents the length of the pilus, x (see Eq. 7). The advantage of presenting the data in this form is that the slope of the curve, dF/dx, directly represents the stiffness of the pilus, k_p. As shown by Schedin et al. (S. Schedin, O. Björnham, M. Andersson, E. Fällman, B. E. Uhlin, and O. Axner, unpublished data), if two or more pili are simultaneously involved in the linear stretching, the

slope of a force-versus-distance curve, as given by Eq. 9, represents the sum of the stiffness for all pili mediating the binding in their first elongation region.

When the force-versus-elongation response is displayed in terms of the position of the large bead, as given by Eq. 8, the corresponding force curves are referred to as force-versus-position curves, whereas when they are displayed in terms of the actual bacterium-to-bead distance, as given by Eq. 9, the corresponding force curves are referred to as force-versus-distance curves.

RESULTS AND DISCUSSION

Verification of pili response

To verify that the force measurements observed were due to an elongation of P pili, a series of control measurements were performed using different bacteria and purified pili. Fig. 6 shows AFM images of HB101/pPAP5 expressing normal length pili (Fig. 6 *A*), and of HB101/pPAN5 expressing shorter and fewer pili on the cell surface (Fig. 6 *B*). The control measurements also encompassed purified pili from HB101/pPAP5 (Fig. 6 *C*). The AFM images were used to confirm sample purity and to determine pili length. The HB101/pPAP5-encoded pili measured 1.44 ± 0.60 μm and the HB101/pPAN5-encoded pili were found to be 0.26 ± 0.10 μm.

Representative OT measurements of typical force curves for pili expressed by HB101/pPAP5 and HB101/pPAN5 bacteria are presented in Fig. 7, *A* and *B*, respectively. A corresponding curve for purified pili is displayed in Fig. 7 *C*. The figure shows first of all that the force-versus-position curves for the HB101/pPAP5 and HB101/pPAN5 bacteria (Fig. 7, *A* and *B*) are of similar general form to that from purified pili (Fig. 7 *C*). Secondly, as will be discussed in some detail below, although the force curves involve a binding partly mediated by more than one pilus, the responses from all three systems are in qualitative agreement with the predictions from the simple model of P pilus elongation presented above in Eq. 1. Thirdly, the force-versus-position curves are shorter for the HB101/pPAN5 than the HB101/pPAP5 bacteria. Inasmuch as the HB101/pPAN5 bacteria have shorter pili than HB101/pPAP5, this is also in agreement with the expected behavior of pili stretching. All these observations constitute a clear confirmation that the measured force-versus-elongation responses indeed originate from P pili and not as a result of a deformation of the anchorage or the outer membrane of the bacterium.

System response for short elongations of a multi-pili binding

The initial regions of the curves displayed in Fig. 7, up to ~1 μm for HB101/pPAP5 (Fig. 7 *A*), ~0.5 μm for the HB101/PAN5 (Fig. 7 *B*), and ~0.1 μm for pure pili (Fig. 7 *C*), (*arrows*) display an increasing (basically linear) force-versus-elongation response. This response is indicative of an elastic linear elongation of pili and concurs therefore with the expected behavior of one or several pili being in region I. However, as was alluded to above, inasmuch as the stiffness of a pilus depends on its length (Eq. 4), several long pili can give rise to a force-versus-position curve that, in the linear region, looks identical to that produced by fewer shorter pili (S. Schedin, O. Björnham, M. Andersson, E. Fällman, B. E. Uhlin, and O. Axner, unpublished data). It is, therefore, in most cases, not possible to unambiguously determine the number of pili (or their stiffness or their lengths) responsible for the binding at each moment in time solely from the first part of a force-versus-position curve.

After some stretching, each pilus mediating the binding proceeds through one of three actions; i), it transitions into its second region of elongation, ii), it detaches from the small bead, or iii), it breaks. As is indicated by the model given above, the system response to a single pilus that makes a transition from region I to region II should, in accordance with Fig. 4, give rise to a force response that is continuous but changes its slope, taking the form of a horizontal curve. The system response from a pilus that detaches, on the other hand, is expected to constitute a sudden decrease of the force, below referred to as a kink in the curve. The system response from a pilus that breaks is expected to be identical to that when one pilus detaches. However, as is shown in a separate work devoted to the contraction behavior of pili (E. Fällman,

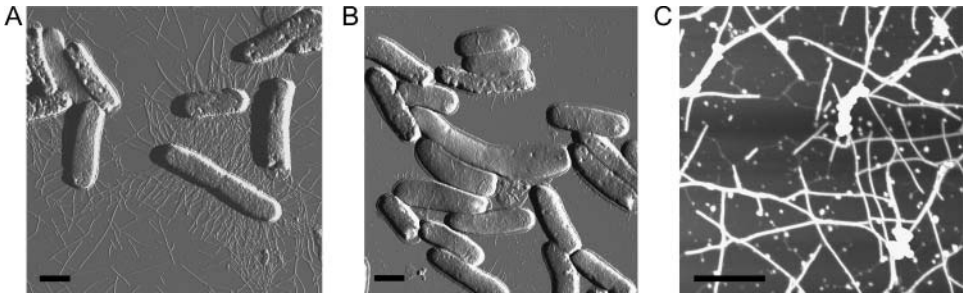

FIGURE 6 Atomic force microscopy images of *E. coli* HB101 with pPAP5 (*A*) and pPAN5 (*B*) and purified pili from HB101/pPAP5 (*C*). The pili were measured from the cell surface edge and an average of 25 measurements was taken. The images in *A* and *B* of the bacteria are presented in amplitude mode of a 10 × 10-μm scan area, whereas the image of the purified pili (*C*) is presented in height mode of a 2 × 2-μm scan area. The scale bar in panels *A* and *B* are 1 μm, whereas that in panel *C* is 0.5 μm.

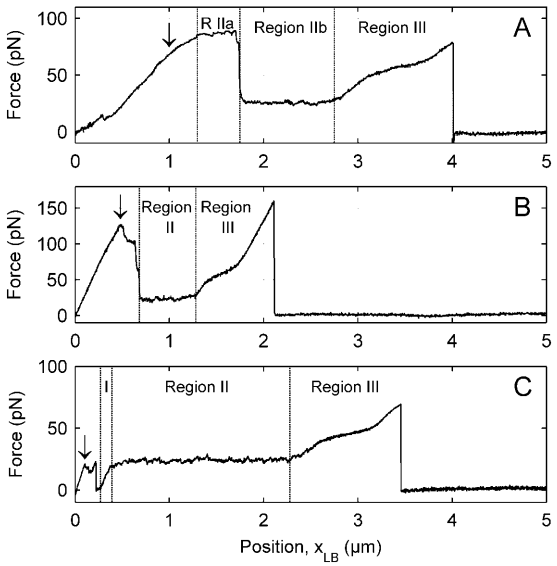

FIGURE 7 Typical force-versus-position curves from three different samples in terms of the position of the large bead showing stretching of the P pili. (*A*) HB101/pPAP5, normal pili; (*B*) HB101/pPAN5, short pili; and (*C*) free (pure) pili. The response of pili from three deformation regions are observed: region I, characterized by a constant slope that indicates a linear elastic elongation of the helical pili-structure; region II, characterized by a constant force indicating unfolding of the PapA rod; and finally region III with a nonlinearly increasing force (s-shaped force-versus-position curve) until the bond ruptures. The parts of the curves in which the remaining pili were all in the same region have been marked with the corresponding region number (I, II, or III).

S. Schedin. J. Jass, B. E. Uhlin, and O. Axner, unpublished data), a pilus detaches rather than breaks when the force becomes sufficiently large. Breaking will therefore not be considered a viable fate of a stretched pilus in this work.

Elongation of a multi-pili binding gives, in general, rise to a combined effect of several single-pilus responses of all the types discussed above. The force response from pili being in their first elongation region can, therefore, sometimes be difficult to interpret in detail. We will here, however, point out the most characteristic force-versus-elongation features of multi-pili binding.

1. Multi-pili binding with pili sequentially making a transition from region I to region II. The system response from a multi-pili binding in which all pili sequentially make a transition from region I to region II is expected to constitute a continuous force-versus-position curve that successively is being transformed from a linear (sloping) curve to a horizontal curve by a rollover-type behavior. An example of such a situation is found for bead positions between 1 and 1.8 μm in Fig. 7 *A*. Inasmuch as the force-versus-position curve is basically horizontal for elongations between 1.2 and 1.8 μm, at a level of $\sim$80 pN, denoted Region IIa in Fig. 7 *A*, no pilus remained in its first elongation region. The lack of sudden kinks for elongations up to 1.8 μm shows that most of the pili that originally mediated the binding in this particular case remained attached and successively made their transition from region I to region II. At an elongation of 1.8 μm, most pili (all except one; see discussion below) detached, which was revealed by the sudden decrease in force.
2. Multi-pili binding with pili sequentially detaching. Two examples of clear evidence of successive detachment of pili are shown in Fig. 8. The first parts of the force-versus-position curves in this figure show that the binding of a HB101/pPAP5 bacterium to a small bead originally was mediated by several pili that successively detached as the binding was stretched. The curves show a stepwise linear force-versus-elongation behavior for short elongations (up to a bead position of $\sim$1 μm) in which the linear responses are separated by a number of kinks (sudden decreases of the force), indicative of pili detachment, which, for example, in Fig. 8 *A* takes place at $\sim$0.15, 0.34, and 0.67 μm (*arrows*). Each kink in a force-versus-position curve thus corresponds to the detachment of one or several pili in a bacterium-to-surface binding mediated by a multi-pili attachment.

In general, both transitions between the two regions (which give rise to a rollover behavior) and detachment (giving rise to kinks) can take place simultaneously or intermittently in elongations of multi-pili bindings. One such example is that given in Fig. 8 *B*, which shows several kinks <1 μm and a rollover behavior up to 1.5 μm. The system response from a multi-pili attachment with pili mainly

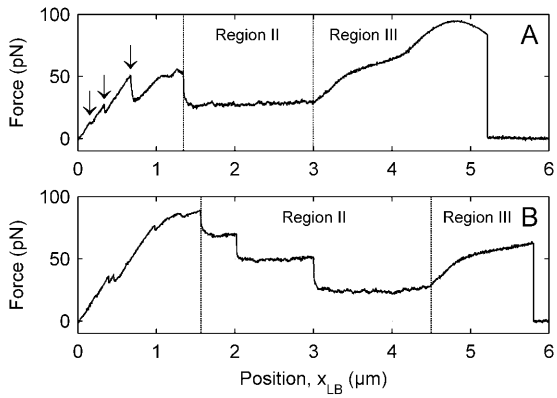

FIGURE 8 Typical force-versus-position curves for multi-pili interaction from two different bacteria in terms of the position of the large bead. (*A*) The first part, displaying a stepwise linear force versus elongation, is indicative of binding mediated by several pili in their elastic region. The discontinuities observed at 0.15, 0.34, and 0.67 μm (*arrows*) are due to rupture of one or several pili. The constant force between 1.3 and 3 μm originates from unfolding of the PapA rod from a single pilus. The force response >3 μm originates from an elongation of the unfolded pilus in its third elongation region. The rollover at $\sim$4.8 μm and above (for forces around and $>$90 pN) originates from a nonlinearity in the force in the position-monitoring instrumentation. (*B*) A similar measurement showing the response from another bacterium. In this situation, three different force levels of unfolding were found, in the intervals 1.6–2 μm, 2–3 μm, and 3–4.5 μm (*arrows*). These levels were found to originate from 3 pili, 2 pili, and 1 pilus being simultaneously in their unfolding region, respectively.

being in region I thus does not solely constitute a simple response as that of a single pilus, but rather a piecewise linear behavior with several kinks and a successive rollover behavior originating from a multi-pili binding. A detailed analysis of the force-versus-elongation response of multi-pili binding in region I is thereby rather complex, and is the subject of evaluation in a separate report (S. Schedin, O. Björnham, M. Andersson, E. Fällman, B. E. Uhlin, and O. Axner, unpublished data).

System response from P pili all simultaneously in region II

The analysis of force curves for pili in the unfolding region (region II) is less complex. When all pili have left their first elongation region (but no one so far has entered its third), the force-versus-elongation response, originating from a binding mediated by one or several pili being in their unfolding region, is, according to the model above, expected to be a horizontal line. Such constant force levels can be found in every curve shown in Figs. 7 and 8. In fact, such constant elongation regions were found in virtually all measurements (except those for which all pili detached very early). This constant force-versus-elongation response in the measurement data support our assumption that the unfolding of the helical (quaternary) structure of the PapA rod takes place in a serial manner and under a constant force. The fact that the signature of a pilus being unfolded is an elongation-independent (constant) force makes it also possible to unambiguously conclude when all binding pili have left their elastic region.

Assessment of unfolding forces of P pili

The force levels at which this unfolding takes place are between 25 and 28 pN for the cases in Fig. 7, *B* and *C*, and Fig. 8 *A*. The data in Fig. 7 *A* and Fig. 8 *B* show a more complex behavior, with more than one constant force level (of which the last ones are in the aforementioned range). The multilevel response of these two figures is consistent with the expected behavior of several pili that unfold simultaneously. Inasmuch as each pilus is expected to yield the same unfolding force, F_{uf}, given by the molecular structure of the PapA rod, data of this kind provide a possibility to determine the force associated with the unfolding of one single pilus as well as the number of pili that unfolded simultaneously.

Fig. 9 displays the distribution of unfolding forces from a large number of measurements ($n \approx 100$) of the types displayed in Figs. 7 and 8. As observed in Fig. 9, the measured unfolding forces cluster into a few ''groups'', roughly of ''integer'' multiples of a minimum unfolding force. The mean values and standard deviation of the unfolding forces in the four groups were found to be 26.7 ± 1.7, 53.5 ± 3.5, 78.7 ± 4.7, and 108 ± 4 pN, respectively. The resolution of the system was estimated to ~1 pN for a few seconds of integration time, which agrees well with the fluctuations in the unfolding forces of curves such as those shown in Fig. 8. Inasmuch as there was no incidence of unfolding forces <20 pN, and the mean values of the four groups relate well to 1:2:3:4, we concluded that the four groups represent binding events mediated by 1, 2, 3, and 4 pili being simultaneously in their unfolding region. The data in Fig. 9 indicate that the unfolding force for a single P pilus is 27 ± 2 pN.

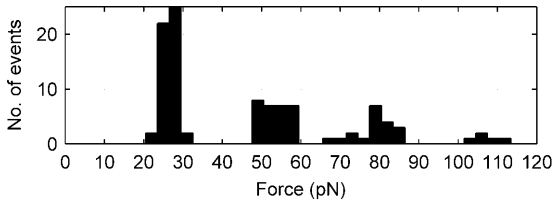

FIGURE 9 Histogram showing the distribution of events of unfolding forces. The four groups represent the constant forces that mediate the binding during simultaneous unfolding of 1, 2, 3, and 4 pili. The mean values of the first, second, third, and fourth group, were found to be 26.7, 53.5, 78.7, and 108 pN, respectively.

Single versus multi-pili response in region II

Based upon the assessment of the unfolding force for a single P pilus, it could be concluded that the pili unfolding that is seen in Fig. 7, *B* and *C*, and in Fig. 8 *A* indeed resulted from only a single pilus. Furthermore, it could be verified that three dissimilar unfolding force levels displayed in Fig. 8 *B* (at extensions of 1.6–2, 2–3, and 3–4.5 μm, respectively) correspond to binding mediated by three, two, and finally one pilus, all simultaneously being in their unfolding regions, but sequentially detaching from the small bead as the bacterium-to-bead distance was increased. A similar explanation can be given for the two unfolding regions in Fig. 7 *A* (corresponding to binding mediated by three and one pilus, respectively). Multi-pili unfolding, with successive pili detachments, as displayed in Fig. 8 *B*, was observed in a large fraction of the studies that served as a basis for the histogram in Fig. 9.

For the cases in Fig. 7, *A* and *B*, as well as in Fig. 8, the elongation-independent force was preceded by a sudden drop in the force curve, indicating the detachment of one or several pili (at ~1.8 μm in Fig. 7 *A*, at ~0.7 μm in Fig. 7 *B*, at ~1.3 μm in Fig. 8 *A*, and ~1.5 μm in Fig. 8 *B*). This gives direct evidence that the former parts of the data correspond to the simultaneous binding of several pili. Conversely, in Fig. 7 *C* the constant force level was preceded by a linear response, starting from the zero level. This shows that the entire response from 0.4 μm and on in Fig. 7 *C* originated from one single pilus.

Inasmuch as Fig. 7 *C* shows the response of one single pilus, all three elongation regions of a single pilus can be explicitly identified in the measurement data. The three

elongation regions of a single pilus are therefore explicitly marked in Fig. 7 *C* for clarity. However, in Fig. 7, *A* and *B*, a single pilus response occurred only after the sudden drop in the force curve (at ~1.8 μm in Fig. 7 *A*, and at ~0.7 μm in Fig. 7 *B*), at which point the remaining pilus had already entered its second elongation region. Only the second and third elongation regions of a P pilus can therefore be identified in these curves. A comparison of the latter part of the force curve in Fig. 7 *C* (from ~0.23 μm and on) with the behavior predicted by the model, displayed in Fig. 4 above, shows that the mathematical model for the force versus elongation of a single pilus given by Eq. 1 is adequate.

System response from P pili being in region III

After stretching at a constant force of ~27 pN for a while (e.g., up until 2.8, 1.3, and 2.3 μm for the three cases displayed in Fig. 7, *A–C*, respectively), the entire PapA rod of the remaining pili eventually became fully unfolded, whereby the pili entered their third region. The elongation that takes place in this region is more complex than in the other regions. As seen from the measurement data in Figs. 7 and 8, which display a transition from region II to region III for a single pilus, the force-versus-position curves have neither a linear, nor a constant, form in region III; qualitatively speaking they have the form of an ''s''.

It is presently conceived that this elongation represents the bending and possibly stretching of the head-to-tail interaction between the adjacent PapA subunits of the unfolded pilus although it cannot be ruled out that it also partly can originate from a stretching of the PapA units themselves. Although more difficult to model, the elongation behavior of a pilus in region III is, however, consistent between various measurements, which, for example, can be seen from a comparison of the curves in Figs. 7 and 8 (the rollover behavior of the force curve in the end of region III in Fig. 8 *A* is due to a nonlinearity in the detection process of the small bead and should therefore not be seen as a deviation from the ''s''-shape that generally appears in region III). Moreover, the length of the force curve in region III is correlated to that of the pili. For the examples displayed in Fig. 7, *A* and *B*, it can be concluded that the ''s''-form displayed in region III is shorter for HB101/pPAN5 (Fig. 7 *B*) than for HB101/pPAP5 (Fig. 7 *A*), relatively well in proportion to the original length of the two pili variants. Measurement data showing several pili making their transition into region III have also been found; however, these generally show a more complex behavior (data not shown). The force dependence in this region will be analyzed in detail in a separate report.

The structural parameters of P pili

As could be concluded from the modeling of a single pilus above, the length-independent structural parameter $(EA)_p$ can be obtained from a measurement in which either the stiffness, k_p, and the natural length, x_0, of the pilus are known, i.e., according to Eq. 4, or the ratio of the unfolding force and the relative elongation in region I are known, given by Eq. 5. Inasmuch as it is not always clear as to how many pili mediate the force in region I, and thereby how many pili contribute to the measured stiffness at any given time, it is not straightforward to determine the value of $(EA)_p$ from Eq. 4 by solely performing a force-versus-elongation measurement in region I. However, by performing a measurement in which the stretching brings the pili into region II without any pili detachment, the number of pili involved in each interaction can be indisputably determined. A value of $(EA)_p$ can then be determined by screening out measurements in which only one pilus mediated the force. When such screening has been performed, $(EA)_p$ can be determined from Eq. 4 when the stiffness, k_p, and the unstretched length, x_0, have been determined.

Three examples of measurements from which the length-independent structural parameter $(EA)_p$ could be determined are given in Fig. 10. The curve in Fig. 10 *A* corresponds to measurements on purified pili, whereas those in Fig. 10, *B* and *C*, originate from HB101/pPAP5. To provide the best conditions for analysis, the data have this time been plotted

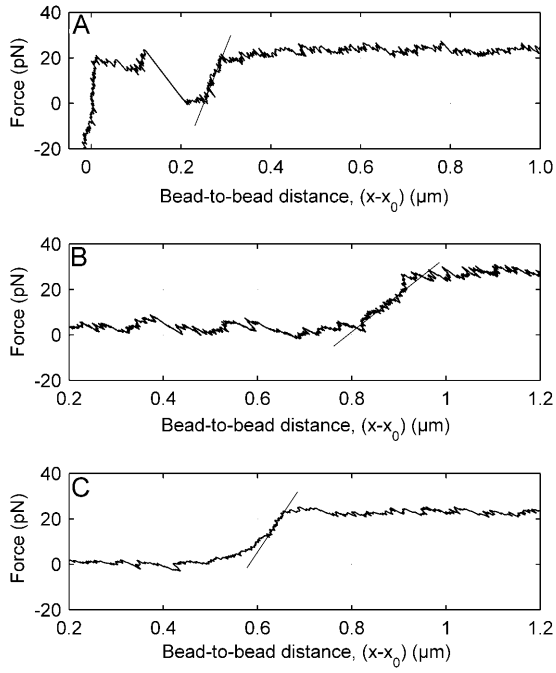

FIGURE 10 Force-versus-distance curves for individual pili displayed as a function of bead-to-bead distance. (*A*) Free (pure) pili; (*B*, *C*) HB101/pPAP5. Panel *A* is constructed from data shown in Fig. 7 *C*, recalculated as a function of the distance between the two beads, i.e., $x - x_0$. The lines represent the slope of each curve and, according to Eq. 9, also the stiffness of each pilus. The position from which the constant force starts to increase from zero represents the unstretched pilus length, x_0. The length-independent structural parameter $(EA)_p$ for a Pap pilus was in these three cases assessed to 150, 144, and 152 ± 20 pN, respectively.

as a function of bond length, $x - x_0$, i.e., the distance between the two beads, according to Eq. 9. Referring to Fig. 10 *A*, the first part of the force-versus-distance curve, up to a bead-pili separation of 0.1 μm, corresponds to a response from one or several loosely bound pili that bind with only a fraction of their normal lengths. At ~0.12 μm, all the force-mediating pili detached. The pili elongated thereby momentarily up to a length of 0.21 μm. The reason for this is that a sudden alteration in the number of pili mediating the force during a measurement affects instantaneously the distance between the beads (the bead in the trap shifts suddenly by a distance given by the ratio of the change in force and the stiffness of the trap). Pili detachment in OT measurements gives, therefore, rise to a discontinuity in the distribution of force-versus-elongation data points, which in turn, when presented as a force-versus-distance curve as in Fig. 10, shows up as a straight, noiseless section.

After the rupture of the initial pilus/pili, no forces were present in the system until the distance between the pili and the bead reached 0.25 μm, when the force again started to increase linearly with distance. This suggests that another pilus, which until this moment had been unstretched, started to elongate elastically at this point. This indicates, in turn, that the length of the part of the pilus that mediates the binding in Fig. 10 had an unstretched length, x_0, of 0.25 $\pm$ 0.01 μm. The stiffness of this pilus was found to be 600 $\pm$ 70 pN/μm. Equation 4 then provides a value for the structural parameter $(EA)_p$ of this particular pilus of 150 $\pm$ 20 pN, where the error given primarily has a systematic origin. A corresponding analysis for the other two curves shows similar $(EA)_p$ values; 144 and 152 $\pm$ 20 pN, respectively. The structural parameter $(EA)_p$ of P pili in region I was found to be 154 $\pm$ 20 pN based upon six separate measurements. The statistical error in the measurements (4 pN) was significantly smaller than the expected systematic error (20 pN).

This value is in reasonable agreement with the structural parameter of 135 pN that can be extracted from the work presented by Bullit and Makowski (1995) using our well-determined value of the unfolding force, F_{uf}, of 27 $\pm$ 2 pN and their value of the relative elongation of P pili, ε_p (x_1), of ~20% using Eq. 5. In addition, our determinations of the structural parameter and the unfolding force of 154 $\pm$ 20 pN and 27 $\pm$ 2 pN, respectively, correspond to a relative elongation of 17.5 $\pm$ 2.5%, which in turn concurs with the value of Bullit and Makowski of ~20% (Bullitt and Makowski, 1995).

Moreover, the elastic elongation continued until the force became independent of elongation, at 0.29 μm, at which point the pilus entered region II, characterized by an elongation-independent force, corresponding to an unfolding of the PapA rod. Although not shown in Fig. 10 *A*, the unfolding of the purified pilus continued up to a distance of 2.19 μm, similar to that of the pili on HB101/pPAP5. This particular pilus, whose unstretched length was 0.25 μm, could thus be elongated 1.94 μm in its unwound region, which corresponds to a relative elongation of ~7.8. The relative elongation for P pili in region II was in general found to be 7 $\pm$ 2. Also this result confirms, in part, the model presented by Bullit and Makowski, which suggested a relative elongation of 5 (Bullitt and Makowski, 1995).

Maximum force mediated by a single pilus

The maximum force sustained by an individual pilus depends on the weakest link in the pilus structure, from the anchor, including the subunit interactions, to the attachment site on the bead. The measurements show a wide distribution of maximum forces. We interpret this as an indication of a large distribution of binding forces of the pili on the small bead rather than as a wide difference in strength of the pili. Moreover, most measurements made for this study were performed using instrumental conditions optimized for highest resolution (i.e., with a small trap stiffness), which implied that the force-versus-deflection response of the trap became nonlinear when the forces exceeded 100 pN. No extensive investigation of the maximum force that a pilus could sustain was therefore undertaken in this study. The experiments performed with higher stiffness indicated, however, that binding interactions can at least reach 200 pN, as is illustrated in Fig. 11 displaying the force response of a HB101/pPAN5 bacterium. The measurements did not demonstrate any major difference in the maximum force for long or short pili, which was in agreement with expectations, inasmuch as the detachment of a pilus is not assumed to depend on its length.

SUMMARY AND CONCLUSIONS

The mechanical properties of P pili from uropathogenic *E. coli* have been investigated using an OT system designed to measure forces of interaction in situ of living biological samples. The system is able to measure forces in the low pN range with high resolution, as well as structural elongation and movement in the low nanometer range. Considerable effort was placed on the calibration of the system. Two independent calibration techniques were used, one based on Brownian motion and the other on Stoke's drag force. The

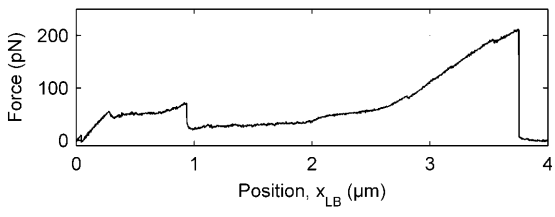

FIGURE 11 An example of force-versus-position curve for a HB101/pPAN5 bacterium that demonstrates a strong binding, with a maximum force at rupture ~200 pN. The power of the laser was 1.5 W.

two agreed to within a few percent (Fällman et al., 2004). We consider the systematic error in the measurements performed to be $<20\%$.

It was assumed that the mechanical properties of P pili are dominated by those of the PapA rod. A model for the elongation of the PapA rod was developed (given by Eq. 1). The agreement between the model and the experimental findings supports the assumption that the mechanical properties of a P pilus are mainly governed by the properties of the PapA rod and that the model given above, Eq. 1, is adequate.

A variety of forces encountered when stretching P pili have been quantitatively evaluated. It was observed that the elongation of the pili took place in three separate regions. In the first region, region I, the pili elongated elastically, with an elongation proportional to the force applied, similar to the elongation of an ideal spring. It was found that the pili could be elongated up to $16 \pm 3\%$ in this region. Although individual pili have different free lengths, and inasmuch as several pili may be stretched simultaneously, it was concluded that it is not appropriate to use the concept of a stiffness (defined as the slope of a force-versus-distance curve in the elastic region) for assessing the elastic properties of an individual pilus. The elasticity is better described by a length-independent material parameter, consisting of the product of an elasticity modulus (Young's modulus, E) and an associated area, A, represented by $(EA)_p$. The value of $(EA)_p$ was found to be 154 ± 20 pN ($n = 6$) for an individual P pilus.

It has been experimentally verified that for a particular length, an individual P pilus performs a transition from an elastic elongation (in which the force is proportional to the elongation) to an elongation under constant force. This region, which has been referred to as region II, was observed as a ''plateau'' in the measurement data. During this phase, the pili unfold their helix structure by a sequential breakage of the interactions between adjacent PapA turns, at a force experimentally determined to 27 ± 2 pN ($n \approx 100$). Examples of situations when one, two, or three pili simultaneously unfolded were encountered. It was also observed that the total elongation for a fully unfolded pilus may be up to 7 ± 2 times its unstretched length. It was finally found that P pili elongate in a nonlinear manner, with an ''s''-shaped form, for elongations beyond that of region II, referred to as region III.

These findings give direct support to the notion that bacterial pili may have intrinsic elongation properties that would allow them to support tension over a broad range of lengths (Bullitt and Makowski, 1995). The possibility of simultaneous and polyvalent binding by several pili that are able to undergo such mechanically induced transitions should presumably be advantageous to bacterial attachment under conditions when they are subject to shear forces as would be encountered in the body.

This project was supported by the Swedish Research Council (Vetenskapsrådet).

REFERENCES

Ashkin, A. 1992. Forces of a single-beam gradient laser trap on a dielectric sphere in the ray optics regime. *Biophys. J.* 61:569–582.

Båga, M., M. Norgren, and S. Normark. 1987. Biogenesis of *E. coli* Pap Pili: PapH, a minor pilin subunit involved in cell anchoring and length modulation. *Cell.* 49:241–251.

Berg-Sorensen, K., and H. Flyvbjerg. 2004. Power spectrum analysis for optical tweezers. *Rev. Sci. Instrum.* 75:594–612.

Berry, R. M., and H. C. Berg. 1997. Absence of a barrier to backwards rotation of the bacterial flagellar motor demonstrated with optical tweezers. *Proc. Natl. Acad. Sci. USA.* 94:14433–14437.

Bullitt, E., C. H. Jones, R. Striker, G. Soto, F. Jacob-Dubuisson, J. Pinkner, M. J. Wick, L. Makowski, and S. J. Hultgren. 1996. Development of pilus organelle subassemblies in vitro depends on chaperone uncapping of a beta zipper. *Proc. Natl. Acad. Sci. USA.* 93:12890–12895.

Bullitt, E., and L. Makowski. 1995. Structural polymorphism of bacterial adhesion pili. *Nature.* 373:164–167.

Bullitt, E., and L. Makowski. 1998. Bacterial adhesion pili are heterologous assemblies of similar subunits. *Biophys. J.* 74:623–632.

Bustamante, C., Z. Bryant, and S. B. Smith. 2003. Ten years of tension: single-molecule DNA mechanics. *Nature.* 421:423–427.

Cappella, B., and G. Dietler. 1999. Force-distance curves by atomic force microscopy. *Surface Science Reports.* 34:1–104.

Chen, A. L., and V. T. Moy. 2002. Single-molecule force measurements. *In* Atomic Force Microscopy in Cell Biology. Academic Press, San Diego, CA. 301–309.

Chen, X., and H. C. Berg. 2000. Torque-speed relationship of the flagellar rotary motor of *Escherichia coli*. *Biophys. J.* 78:1036–1041.

Fällman, E., and O. Axner. 1997. Design for fully steerable dual-trap optical tweezers. *Appl. Opt.* 36:2107–2113.

Fällman, E., S. Schedin, J. Jass, M. Andersson, B. E. Uhlin, and O. Axner. 2004. Optical tweezers based force measurement system for quantitating binding interactions: system design and application for the study of bacterial adhesion. *Biosens. Bioelectron.* 19:1429–1437.

Gallet, F. 2004. Applications of optical tweezers and microspheres for the micromanipulation of biomolecules and cells. *Ann. Biol. Clin.* 62:85–86.

Giocondi, M. C., P. E. Milhiet, E. Lesniewska, and C. Le Grimellec. 2003. From cell imaging to molecular manipulation: biological applications of atomic force microscopy. *Med. Sci.* 19:92–99.

Gong, M. F., and L. Makowski. 1990. Structural studies of Pap pili from *Escherichia coli*. *Biophys. J.* 57:254a. (Abstr.).

Gong, M. F., and L. Makowski. 1992. Helical structure of P-pili from *Escherichia coli*: evidence from x-ray fiber diffraction and scanning-transmission electron-microscopy. *J. Mol. Biol.* 228:735–742.

Gong, M. F., J. Wall, H. S. Batliwala, and L. Makowski. 1992. Structural studies of Pap adhesion pili from *Escherichia coli*. *FASEB J.* 6:471a. (Abstr.).

Hansma, H. G., and L. Pietrasanta. 1998. Atomic force microscopy and other scanning probe microscopies. *Curr. Opin. Chem. Biol.* 2:579–584.

Ikai, A., and R. Afrin. 2003. Toward mechanical manipulations of cell membranes and membrane proteins using an atomic force microscope: an invited review. *Cell Biochem. Biophys.* 39:257–277.

Jacob-Dubuisson, F., J. Heuser, K. Dodson, S. Normark, and S. Hultgren. 1993. Initiation of assembly and association of the structural elements of a bacterial pilus depend on two specialized tip proteins. *EMBO J.* 12: 837–847.

Johnson, J. R., and T. A. Russo. 2002. Uropathogenic *Escherichia coli* as agents of diverse non-urinary tract extraintestinal infections. *J. Infect. Dis.* 186:859–864.

Källenius, G., S. B. Svenson, H. Hultberg, R. Möllby, I. Helin, B. Cedergren, and J. Winberg. 1981. Occurrence of P-fimbriated *Escherichia coli* in urinary tract infections. *Lancet.* 2:1369–1372.

Kuehn, M. J., J. Heuser, S. Normark, and S. J. Hultgren. 1992. P pili in uropathogenic *Escherichia coli* are composite fibers with distinct fibrillar adhesive tips. *Nature*. 356:252–255.

Kumar, S., and J. H. Hoh. 2001. Probing the machinery of intracellular trafficking with the atomic force microscope. *Traffic*. 2:746–756.

Kuo, S. C. 2001. Using optics to measure biological forces and mechanics. *Traffic*. 2:757–763.

Kuyper, C. L., and D. T. Chiu. 2002. Optical trapping: a versatile technique for biomanipulation. *Appl. Spectrosc.* 56:300A–312A.

Leckband, D. 2000. Measuring the forces that control protein interactions. *Annu. Rev. Biophys. Biomol. Struct.* 29:1–26.

Leckband, D., and J. Israelachvili. 2001. Intermolecular forces in biology. *Q. Rev. Biophys.* 34:105–267.

Liang, M. N., S. P. Schmith, S. J. Metallo, I. S. Choi, M. Prentiss, and G. M. Whitesides. 2000. Measuring the forces involved in polyvalent adhesion of uropathogenic *Escherichia coli* to mannose-presenting surfaces. *Proc. Natl. Acad. Sci. USA*. 97:13092–13096.

Lindberg, F., B. Lund, L. Johansson, and S. Normark. 1987. Localization of the receptor-binding protein adhesin at the tip of the bacterial pilus. *Nature*. 328:84–87.

Lindberg, F., B. Lund, and S. Normark. 1986. Gene products specifying adhesion of uropathogenic *Escherichia coli* are minor components of pili. *Proc. Natl. Acad. Sci. USA*. 83:1891–1895.

Lindberg, F. P., B. Lund, and S. Normark. 1984. Genes of pyelonephritogenic *E. coli* required for digalactoside-specific agglutination of human cells. *EMBO J.* 3:1167–1173.

Maier, B., L. Potter, M. So, H. S. Seifert, and M. P. Sheetz. 2002. Single pilus motor forces exceed 100 pN. *Proc. Natl. Acad. Sci. USA*. 99: 16012–16017.

Merkel, R. 2001. Force spectroscopy on single passive biomolecules and single biomolecular bonds. *Phys. Rep.* 346:344–385.

Merz, A. J., M. So, and M. P. Sheetz. 2000. Pilus retraction powers bacterial twitching motility. *Nature*. 407:98–102.

Nilsson, P., S. Naureckiene, and B. E. Uhlin. 1996. Mutations affecting mRNA processing and fimbrial biogenesis in the *Escherichia coli* pap operon. *J. Bacteriol.* 178:683–690.

Otto, K., H. Elwing, and M. Hermansson. 1999. Effect of ionic strength on initial interactions of *Escherichia coli* with surfaces, studied on-line by a novel quartz crystal microbalance technique. *J. Bacteriol.* 181:5210–5218.

Rice, S. E., T. J. Purcell, and J. A. Spudich. 2003. Building and using optical traps to study properties of molecular motors. *Methods Enzymol.* 361:112–133.

Russo, T. A., and J. R. Johnson. 2003. Medical and economic impact of extraintestinal infections due to *Escherichia coli*: focus on an increasingly important endemic problem. *Microbes Infect.* 5:449–456.

Staros, J. V., R. W. Wright, and D. M. Swingle. 1986. Enhancement by N-hydroxysulfosuccinimide of water-soluble carbodiimide-mediated coupling reactions. *Anal. Biochem.* 156:220–222.

Stolz, M., D. Stoffler, U. Aebi, and C. Goldsbury. 2000. Monitoring biomolecular interactions by time-lapse atomic force microscopy. *J. Struct. Biol.* 131:171–180.

Svoboda, K., and S. M. Block. 1994. Biological applications of optical forces. *Annu. Rev. Biophys. Biomol. Struct.* 23:247–285.

Tromas, C., and R. Garcia. 2002. Interaction forces with carbohydrates measured by atomic force microscopy. *Top. Curr. Chem.* 218:115–132.

Willemsen, O. H., M. M. E. Snel, A. Cambi, J. Greve, B. G. De Grooth, and C. G. Figdor. 2000. Biomolecular interactions measured by atomic force microscopy. *Biophys. J.* 79:3267–3281.

Zlatanova, J., S. M. Lindsay, and S. H. Leuba. 2000. Single molecule force spectroscopy in biology using the atomic force microscope. *Prog. Biophys. Mol. Biol.* 74:37–61.